JACS
JOURNAL OF THE AMERICAN CHEMICAL SOCIETY
Article
Cite This: J. Am. Chem. Soc. 2018, 140, 17591−17596
pubs.acs.org/JACS

Tunable Metal−Organic Frameworks Enable High-Efficiency Cascaded Adsorption Heat Pumps

Adam J. Rieth,[†] Ashley M. Wright,[†] Sameer Rao,[‡] Hyunho Kim,[‡] Alina D. LaPotin,[‡] Evelyn N. Wang,[‡] and Mircea Dincă*[,†]

[†]Department of Chemistry, Massachusetts Institute of Technology, 77 Massachusetts Avenue, Cambridge, Massachusetts 02139, United States

[‡]Department of Mechanical Engineering, Massachusetts Institute of Technology, 77 Massachusetts Avenue, Cambridge, Massachusetts 02139, United States

Supporting Information

ABSTRACT: Rising global standards of living coupled to the recent agreement to eliminate hydrofluorocarbon refrigerants are creating intense pressure to develop more sustainable climate control systems. In this vein, the use of water as the refrigerant in adsorption heat pumps is highly attractive, but such adsorption systems are constrained to large size and poor efficiency by the characteristics of currently employed water sorbents. Here we demonstrate control of the relative humidity of water uptake by modulating the pore size in a family of isoreticular triazolate metal−organic frameworks. Using this method, we identify a pair of materials with stepped, nonoverlapping water isotherms that can function in tandem to provide continuous cooling with a record ideal coefficient of performance of 1.63. Additionally, when used in a single-stage heat pump, the microporous Ni_2Cl_2BBTA has the largest working capacity of any material capable of generating a 25 °C difference between ambient and chiller output.

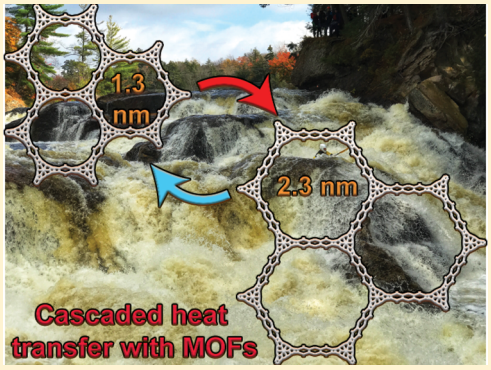

INTRODUCTION

More than 44% of all primary energy in the U.S. residential and commercial sectors is consumed by climate control systems.[1] Globally, as standards of living in the developing world rise, the resultant rapid growth in demand for air conditioning is a major driver of increased worldwide electricity consumption.[2] Thermally driven cooling cycles, such as adsorption heat pumps (AHPs), can utilize previously wasted energy resources such as engine exhaust, waste heat from power generation, or chemical process heat, resulting in dramatic reductions in primary energy consumption for heating and cooling.[3−5] Interest in AHPs using water as the refrigerant has spiked in light of the recent agreement to phase out hydrofluorocarbons, the refrigerants most commonly employed in conventional vapor compression heat pumps, due to their very high global warming potential.[6−8]

Widespread deployment of AHPs is limited by shortcomings of the currently employed active sorbents, including low water capacity and shallow water uptake step profiles that are not tunable as a function of relative humidity (RH).[3,9−12] These shortcomings result in bulky devices that suffer from low thermal efficiency. In principle, the efficiency of AHP systems, as measured by the coefficient of performance (COP), defined as the cooling energy per unit energy input, could be improved by employing multiple-effect cascaded cycles wherein two or more adsorbent beds are operated in series.[13] Cascaded temperature stages allow for the reuse of input thermal energy at progressively lower temperatures in each successive bed, resulting in higher overall efficiency. For instance, a three-stage cascaded AHP using silica gel and activated carbon adsorbents can achieve a superb overall COP of 1 but requires an elevated driving temperature of 220 °C as well as two working fluids, which significantly increases system complexity.[14] Further improvements require designing pairs of materials with water uptake steps tailored to fully reuse the excess energy from the high-temperature stage with the low-temperature stage. Such rational design of adsorbent materials to enable the reuse of input thermal energy twice while employing a single working fluid has not yet been demonstrated.

In view of their recently demonstrated utility as sorbents in AHPs,[4,9,10,15,16] metal−organic frameworks (MOFs) are poised to offer thermodynamically matched material pairs that would enable record performance in cascaded systems. In addition to higher overall capacity, MOFs typically exhibit steeper uptake steps, occurring in a narrow RH range, which directly improve efficiency because cycling between the filled state and the empty state requires a minimal temperature swing.[17] Most importantly for cascaded AHPs, MOFs allow for precise control over the position of water uptake as a function of RH.[11,18−26] This is vital because it determines the maximum temperature difference (lift) an AHP system can produce and

Received: September 6, 2018
Published: November 21, 2018

DOI: 10.1021/jacs.8b09655
J. Am. Chem. Soc. 2018, 140, 17591−17596

defines the required driving temperature to regenerate the sorbent.[9] More hydrophilic sorbents will adsorb water at lower RH and can produce a higher lift but will also require a higher temperature heat source for regeneration because water is adsorbed more strongly. Therefore, the ideal sorbent is one whose hydrophilicity provides enough driving force to achieve the target temperature lift but is not so high as to decrease thermal efficiency.[9,16]

We recently reported a MOF, Co_2Cl_2BTDD (BTDD = bis(1*H*-1,2,3-triazolo[4,5-*b*],[4′,5′-*i*])dibenzo[1,4]dioxin) whose pore size allows water sorption at the uptake reversibility limit.[16,27] Co_2Cl_2BTDD is the best-performing sorbent for single-stage AHPs capable of a 20 °C lift.[9,16] Here we show that a smaller pore isoreticular MOF made from the shorter bistriazolate linker 1*H*,5*H*-benzo(1,2-*d*),(4,5-*d*′)-bistriazole (BBTA)[28,29] is significantly more hydrophilic and enables a lift >40 °C, which, in combination with the larger pore system, can enable a record high-efficiency (COP > 1) cascaded double-effect AHP system (Figure 1).

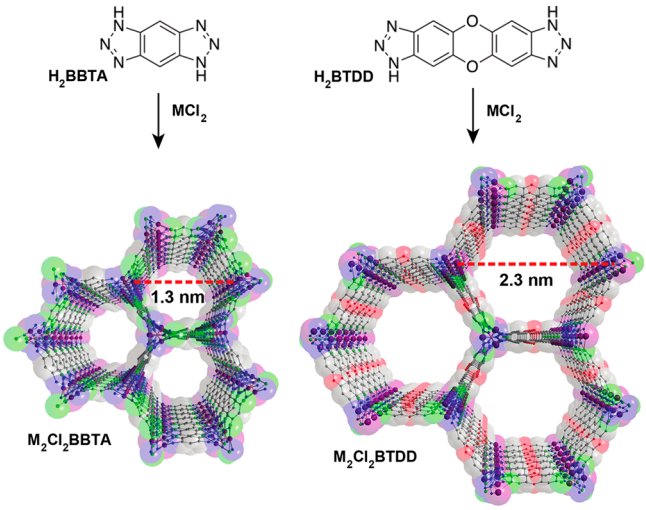

Figure 1. Synthetic route and structure depiction of M_2Cl_2BBTA and M_2Cl_2BTDD. C, gray; O, red; N, blue; Cl, green; M, purple. For clarity, H atoms are omitted.

RESULTS AND DISCUSSION

Water vapor adsorption isotherms measured at 298 K for activated samples of M_2Cl_2BBTA (M = Co, Ni, Cu) are shown in Figure 2. All three materials exhibit type I isotherms as a result of the initial coordination of water to the open metal sites (evidenced by infrared (IR) spectroscopy, Figure S1), followed by further hydrogen-bonding-assisted adsorption until pore saturation at low RH. The nickel and cobalt materials both adsorb nearly 30% water by weight (wt %) below 5% RH. The copper analog exhibits a significantly lower water capacity as well as an irreversible step at 30% RH. Powder X-ray diffraction (PXRD) analysis and nitrogen adsorption experiments revealed that the copper material loses porosity and undergoes a phase change after water uptake (Figures S2 and S3). Similarly, the cobalt material largely maintains its crystallinity but loses much of its porosity after reactivation upon water sorption (Figures S4 and S5). By contrast, the nickel MOF retains its crystallinity and porosity (Figures S6 and S7) even after water sorption and desorption. This stability trend is in line with that previously observed for ammonia

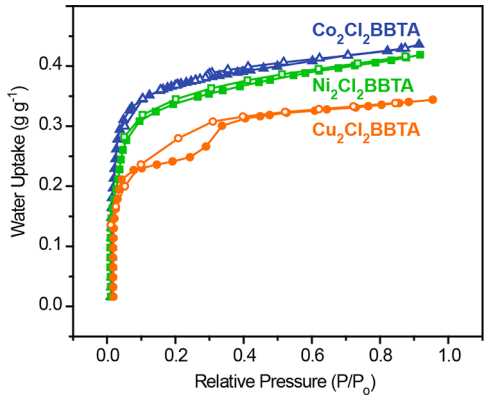

Figure 2. Water vapor isotherms for M_2Cl_2BBTA materials. Adsorption (filled symbols) and desorption (open symbols) at 298 K for Co_2Cl_2BBTA (blue triangles), Ni_2Cl_2BBTA (green squares, measured at 296 K), and Cu_2Cl_2BBTA (orange circles).

sorption in this family of materials and is the result of the kinetics of ligand exchange at the metal ion.[30]

Because of its greater stability, Ni_2Cl_2BBTA would be the more appropriate choice for a cascaded AHP. The enthalpy of water adsorption (ΔH_{ads}) in Ni_2Cl_2BBTA, determined by variable-temperature water vapor sorption isotherms (Figure S8), is ∼55 kJ mol^{-1} at zero coverage, nearly identical to that found for water binding to the open coordination sites of Co_2Cl_2BTDD[16] (Figure S9). Importantly, during pore filling of Ni_2Cl_2BBTA, ΔH_{ads} remains above 50 kJ mol^{-1}, indicating stronger across-pore hydrogen-bonding interactions, likely due to confinement effects,[31,32] than those found in the larger pore Co_2Cl_2BTDD, wherein ΔH_{ads} during pore filling is 46 kJ mol^{-1}. The variable-temperature water vapor isotherms for Ni_2Cl_2BBTA were also used to validate a characteristic curve (Figure S10), which converts the two independent variables that govern uptake, vapor pressure and temperature, into a single parameter related to the Gibbs free energy of adsorption (see the Supporting Information)[9,15,16] and allows extrapolation of the water loading at any temperature and pressure (Figure S11).

Single-Stage Heat Pump Using Ni_2Cl_2BBTA. The characteristic curve can be used to calculate water loadings in Ni_2Cl_2BBTA under conditions relevant for heat pump applications, which are, in turn, used to calculate the working capacity and COP. Under Refrigeration II conditions (i.e., chiller output of 278 K and ambient of 303 K for 25 °C lift),[9] Ni_2Cl_2BBTA has a maximum COP of 0.70 and a volumetric working capacity of nearly 0.40 mL of H_2O mL^{-1} MOF using a 400 K desorption temperature (Figure 3A, filled squares). This is the highest reported volumetric working capacity for any material working under Refrigeration II standardized conditions (i.e., capable of a 25 °C lift). Notably, because of the exceptional hydrophilicity of Ni_2Cl_2BBTA, the temperature lift it could achieve is primarily limited by the regeneration temperature rather than the position of its water uptake step, which is otherwise dominant in other materials. For instance, if the ambient temperature increases to 313 K, then the water–Ni_2Cl_2BBTA working pair can still produce a 278 K chiller output (35 °C lift) with only minimal decreases in the COP and working capacity (Figure 3A, open squares). Furthermore, with an ambient temperature of 30 °C (303 K), Ni_2Cl_2BBTA can achieve a 30 °C lift (Figure 3B, filled green squares), and with an ambient temperature of 40 °C (313 K), Ni_2Cl_2BBTA

DOI: 10.1021/jacs.8b09655
J. Am. Chem. Soc. 2018, 140, 17591−17596

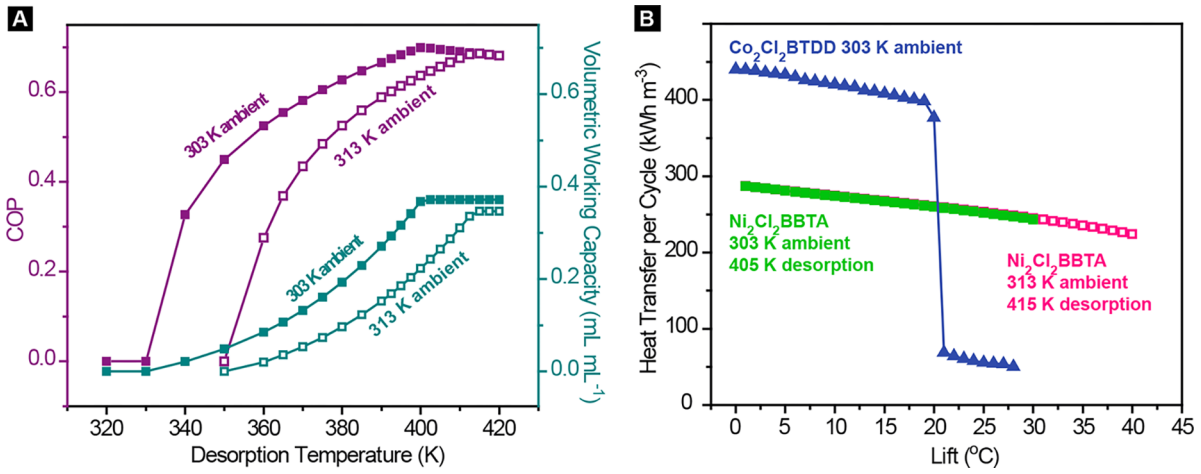

Figure 3. (A) Coefficient of performance (purple symbols, left axis) and volumetric working capacity (aqua symbols, right axis) for Ni_2Cl_2BBTA with a chiller output temperature of 278 K and an ambient temperature of either 303 K (filled symbols, 25 °C lift) or 313 K (open symbols, 35 °C lift) as a function of desorption temperature. (B) Heat transferred per cycle, determined by varying the evaporator (output) temperature, versus temperature lift for Ni_2Cl_2BBTA (squares) and Co_2Cl_2BTDD (blue triangles).

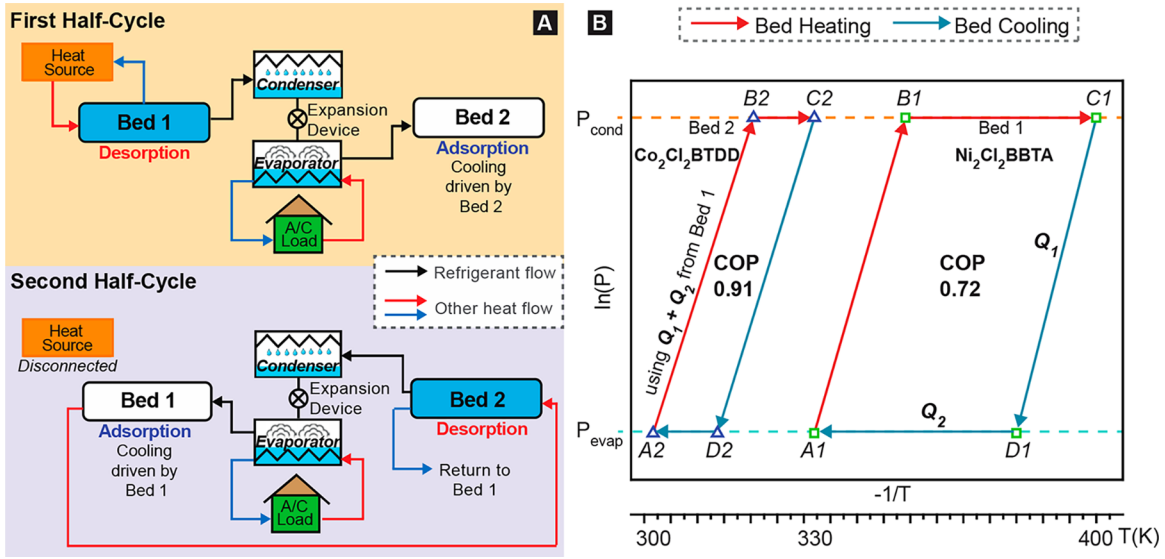

Figure 4. (A) Schematic of a cascaded double-effect adsorption heat pump for stationary applications. (B) Isosteric cycle diagram of a cascaded adsorption heat pump cycle providing a 17 °C lift with evaporator at 283 K, condenser at 300 K, desorption of Co_2Cl_2BTDD at 330 K and desorption of Ni_2Cl_2BBTA at 400 K.

can achieve a 40 °C lift with only a 10 °C increase in desorption temperature (Figure 3B, open pink squares).

In agreement with the characteristic curve calculations, cycling of Ni_2Cl_2BBTA between 25 and 150 °C at a constant vapor pressure of 4.76 mmHg (20% RH at 25 °C, well beyond the saturation RH value at this temperature) revealed an initial slight decline in uptake, followed by a plateau at 0.36 g g^{-1} (Figure S12). We note that this is close to the vapor pressure of water ice at 0 °C, 4.585 mmHg (~20% RH at 25 °C). Impressively, nearly all of the capacity of Ni_2Cl_2BBTA, >0.33 g g^{-1}, is reached below this vapor pressure (Figure 2). Although using water as the refrigerant makes it impossible to cool below 0 °C, the unique behavior of Ni_2Cl_2BBTA toward water vapor highlights its potential as a desiccant in other applications such as industrial compressed air drying that require subzero dewpoints.[33]

Two-Stage Cascaded Heat Pump Using Ni_2Cl_2BBTA and Co_2Cl_2BTDD. To utilize the full potential driving force for heat transfer with Ni_2Cl_2BBTA, we devised a concept tandem cascaded heat pump cycle (Figure 4A,B). Because of the material's exceptional affinity for water, water vapor can be adsorbed from a low-temperature evaporator onto a bed of Ni_2Cl_2BBTA maintained between 104 and 57 °C.

When combined in a tandem cycle with a material exhibiting a lower affinity for water vapor, for instance, the larger pore Co_2Cl_2BTDD, the sensible heat (Q_1) as well as the energy from ΔH_{ads}(Q_2) in the small-pore Ni_2Cl_2BBTA (Bed 1) at elevated temperature can be used to completely regenerate the larger pore Co_2Cl_2BTDD (Bed 2). Both adsorbent beds can be paired with the same evaporator and condenser at temperatures of 10 and 27 °C, respectively (17 °C lift). The minimum adsorption temperature of Bed 2 (Co_2Cl_2BTDD) would be that of the condenser, 27 °C, and it would be regenerated at 57 °C with waste heat from Bed 1 (Ni_2Cl_2BBTA). In turn, Bed 1 would operate at a minimum adsorption temperature of 57 °C and be regenerated by an external heat source at 127 °C. This

DOI: 10.1021/jacs.8b09655
J. Am. Chem. Soc. 2018, 140, 17591−17596

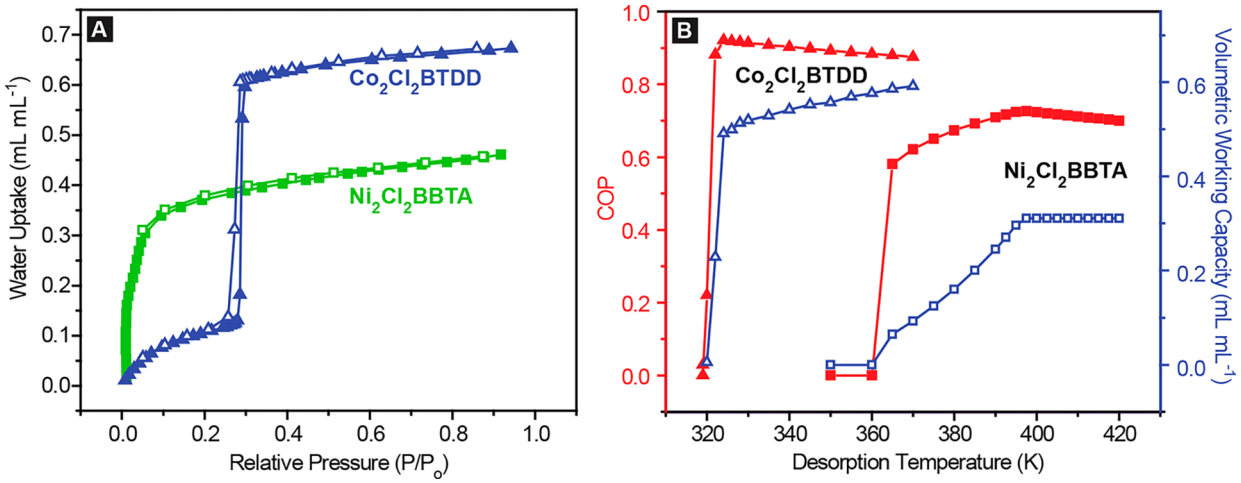

Figure 5. (A) Water vapor adsorption (filled symbols) and desorption (open symbols) in volumetric units at 298 K for Co_2Cl_2BTDD (blue triangles) and Ni_2Cl_2BBTA (green squares). (B) Coefficient of Performance (red filled symbols, left axis) and volumetric working capacity (blue empty symbols, right axis) for Co_2Cl_2BTDD (triangles) and Ni_2Cl_2BBTA (squares) using an evaporator temperature of 283 K and an ambient temperature of 300 K, with a minimum bed temperature during adsorption of 330 K for Ni_2Cl_2BBTA, as a function of desorption temperature.

configuration is ideal for the application of district air conditioning for buildings (Figure 4A).

Altogether, Ni_2Cl_2BBTA and Co_2Cl_2BTDD combine for a cascaded double-effect AHP cycle in which the input thermal energy for regeneration is effectively used twice, once at 127 °C to regenerate the small-pore MOF and again at 57 °C to regenerate the large-pore MOF. In this tandem configuration, Co_2Cl_2BTDD has a working capacity of 0.52 mL mL^{-1} and a COP of 0.91 when regenerated at 57 °C, whereas Ni_2Cl_2BBTA has a working capacity of 0.31 mL mL^{-1} and a COP of 0.72 when regenerated at 127 °C (Figure 5B). Because the COP of the cascading pump is the sum of the COPs for the constituent cycles, the ideal system COP for the combination presented here is 1.63.

The thermodynamic cycle is diagrammed in process flow in Figure 4A and in a tandem isosteric cycle in Figure 4B. Beginning with a saturated bed of Ni_2Cl_2BBTA (Bed 1, point *A1*) and an empty bed of Co_2Cl_2BTDD (Bed 2, point *C2*), Bed 1 undergoes isosteric heating to point *B1*, and its vapor pressure increases from 9.5 mmHg (the pressure of the evaporator) to 26.6 mmHg (the pressure of the condenser). At the same time, Bed 2 undergoes isosteric cooling from point *C2* to point *D2*. Subsequently, Bed 1 is further heated while connected to the condenser for isobaric desorption to point *C1*, whereas Bed 2 is connected to the evaporator and undergoes isobaric adsorption to point *A2*. At this point, the roles of the beds reverse in the second half cycle (Figure 4A). Bed 1 is cooled isosterically to point *D1*, connected to the evaporator, and undergoes isobaric adsorption back to *A1*, whereas the sensible heat $\mathbf{Q_1}$ and the heat of adsorption $\mathbf{Q_2}$ from this process are used to regenerate Bed 2, moving from *A2* to *B2* and finally *C2* (Figure 4B).

The pair of Ni_2Cl_2BBTA and Co_2Cl_2BTDD is the first example of materials with thermodynamically tuned, steep, and nonoverlapping water isotherms (Figure 5A) employed in a cascaded adsorption cycle, which enables significantly greater thermal efficiency by reducing the required temperature swings and minimizing the dead thermal mass. For example, using conventional sorbents, which, due to overlapping isotherms necessitate employing different refrigerants for each stage, an AHP with a cooling COP of 1 requires a three-stage cascade with a source temperature of 220 °C (Table S1).[14] Additionally, previous screening of sorbent–sorbate pairs for tandem heat pumps found theoretical maxima for COP of 1.15 for a tandem activated carbon–methanol and zeolite–water cycle.[13] By contrast, using MOFs with stepped water isotherms tuned by pore size, we demonstrate a record ideal COP of 1.63, >150% higher than the previous best, while notably decreasing system complexity by using water as the sole refrigerant and employing a much lower source temperature of 127 °C.

CONCLUSIONS

Triazolate MOFs are uniquely suited to water vapor isotherm engineering by virtue of their exceptional stability as well as their hydrophilic chains of metals exhibiting open-coordination sites. The microporous BBTA MOFs adsorb water vapor near 0% RH. This unusually high hydrophilicity engenders a high driving force for heat transfer. Compared with other materials capable of generating a 25 °C lift, Ni_2Cl_2BBTA has the greatest uptake capacity and positions it as a key material for the hot adsorption bed of a cascaded AHP. The rational tuning of the water adsorption uptake step enables the design of a pair of complementary materials that can reuse input thermal energy twice while using water as the sole refrigerant. When used in tandem, Ni_2Cl_2BBTA and Co_2Cl_2BTDD combine for an unprecedented COP of 1.63, which can be achieved using an accessible low driving temperature of only 127 °C. The ability to provide continuous cooling with simultaneously high COP, low source temperatures, and using water as the sole refrigerant is a significant advance over the state-of-the-art. This work moves sustainable AHPs using water as a refrigerant closer to widespread adoption.

ASSOCIATED CONTENT

Supporting Information

The Supporting Information is available free of charge on the ACS Publications website at DOI: 10.1021/jacs.8b09655.

Experimental procedures, Table S1, and Figures S1–S12 (PDF)

The authors declare no competing financial interest.

DOI: 10.1021/jacs.8b09655
J. Am. Chem. Soc. 2018, 140, 17591–17596

AUTHOR INFORMATION

Corresponding Author

*mdinca@mit.edu

ORCID

Adam J. Rieth: 0000-0002-9890-1346
Ashley M. Wright: 0000-0002-9475-2638
Evelyn N. Wang: 0000-0001-7045-1200
Mircea Dincă: 0000-0002-1262-1264

Notes

The authors declare no competing financial interest.

ACKNOWLEDGMENTS

Studies of small-molecule interactions with metal nodes in MOFs are supported through a CAREER grant from the National Science Foundation to M.D. (DMR-1452612). A.J.R. is supported by the MIT Tata Center for Technology and Design. We thank the Abdul Latif Jameel World Water and Food Security Lab for Seed funding for water capture. A.J.R. and M.D. are inventors on a patent pertaining to the materials discussed herein.

REFERENCES

(1) U.S. Energy Information Agency. *Annual Energy Outlook 2015 with Projections to 2040*; Washington, DC, 2015.

(2) Reese, A. Slow Coolant Phaseout Could Worsen Warming: As Countries Crank up the AC, Emissions of Potent Greenhouse Gases Are Likely to Skyrocket. *Science* **2018**, *359* (6380), 1084.

(3) Critoph, R. E. Evaluation of Alternative Refrigerant-Adsorbent Pairs for Refrigeration Cycles. *Appl. Therm. Eng.* **1996**, *16* (11), 891–900.

(4) Jeremias, F.; Fröhlich, D.; Janiak, C.; Henninger, S. K. Advancement of Sorption-Based Heat Transformation by a Metal Coating of Highly-Stable, Hydrophilic Aluminium Fumarate MOF. *RSC Adv.* **2014**, *4* (46), 24073.

(5) Narayanan, S.; Yang, S.; Kim, H.; Wang, E. N. Optimization of Adsorption Processes for Climate Control and Thermal Energy Storage. *Int. J. Heat Mass Transfer* **2014**, *77*, 288–300.

(6) Greenblatt, J. B.; Wei, M. Assessment of the Climate Commitments and Additional Mitigation Policies of the United States. *Nat. Clim. Change* **2016**, *6* (12), 1090–1093.

(7) Shine, K. P.; Sturges, W. T. CO_2 Is Not the Only Gas. *Science* **2007**, *315* (5820), 1804–1805.

(8) McLinden, M. O.; Brown, J. S.; Brignoli, R.; Kazakov, A. F.; Domanski, P. A. Limited Options for Low-Global-Warming-Potential Refrigerants. *Nat. Commun.* **2017**, *8*, 14476.

(9) De Lange, M. F.; Verouden, K. J. F. M.; Vlugt, T. J. H.; Gascon, J.; Kapteijn, F. Adsorption-Driven Heat Pumps: The Potential of Metal-Organic Frameworks. *Chem. Rev.* **2015**, *115* (22), 12205–12250.

(10) Ehrenmann, J.; Henninger, S. K.; Janiak, C. Water Adsorption Characteristics of MIL-101 for Heat-Transformation Applications of MOFs. *Eur. J. Inorg. Chem.* **2011**, *2011* (4), 471–474.

(11) Canivet, J.; Bonnefoy, J.; Daniel, C.; Legrand, A.; Coasne, B.; Farrusseng, D. Structure–Property Relationships of Water Adsorption in Metal–Organic Frameworks. *New J. Chem.* **2014**, *38* (7), 3102.

(12) Küsgens, P.; Rose, M.; Senkovska, I.; Fröde, H.; Henschel, A.; Siegle, S.; Kaskel, S. Characterization of Metal-Organic Frameworks by Water Adsorption. *Microporous Mesoporous Mater.* **2009**, *120* (3), 325–330.

(13) Meunier, F. Theoretical Performances of Solid Adsorbent Cascading Cycles Using the Zeolite-Water and Active Carbon-Methanol Pairs: Four Case Studies. *J. Heat Recovery Syst.* **1986**, *6* (6), 491–498.

(14) Douss, N.; Meunier, F. Experimental Study of Cascading Adsorption Cycles. *Chem. Eng. Sci.* **1989**, *44* (2), 225–235.

(15) Cadiau, A.; Lee, J. S.; Damasceno Borges, D.; Fabry, P.; Devic, T.; Wharmby, M. T.; Martineau, C.; Foucher, D.; Taulelle, F.; Jun, C. H.; Hwang, Y. K.; Stock, N.; De Lange, M. F.; Kapteijn, F.; Gascon, J.; Maurin, G.; Chang, J. S.; Serre, C. Design of Hydrophilic Metal Organic Framework Water Adsorbents for Heat Reallocation. *Adv. Mater.* **2015**, *27* (32), 4775–4780.

(16) Rieth, A. J.; Yang, S.; Wang, E. N.; Dincă, M. Record Atmospheric Fresh Water Capture and Heat Transfer with a Material Operating at the Water Uptake Reversibility Limit. *ACS Cent. Sci.* **2017**, *3* (6), 668–672.

(17) Jeremias, F.; Khutia, A.; Henninger, S. K.; Janiak, C. MIL-100(Al, Fe) as Water Adsorbents for Heat Transformation Purposes—a Promising Application. *J. Mater. Chem.* **2012**, *22* (20), 10148.

(18) Wade, C. R.; Corrales-Sanchez, T.; Narayan, T. C.; Dincă, M. Postsynthetic Tuning of Hydrophilicity in Pyrazolate MOFs to Modulate Water Adsorption Properties. *Energy Environ. Sci.* **2013**, *6* (7), 2172.

(19) Wright, A. M.; Rieth, A. J.; Yang, S.; Wang, E.; Dinca, M. Precise Control of Pore Hydrophilicity Enabled by Post-Synthetic Cation Exchange in Metal-Organic Frameworks. *Chem. Sci.* **2018**, *9*, 3856.

(20) Akiyama, G.; Matsuda, R.; Sato, H.; Hori, A.; Takata, M.; Kitagawa, S. Effect of Functional Groups in MIL-101 on Water Sorption Behavior. *Microporous Mesoporous Mater.* **2012**, *157*, 89–93.

(21) Jeremias, F.; Lozan, V.; Henninger, S. K.; Janiak, C. Programming MOFs for Water Sorption: Amino-Functionalized MIL-125 and UiO-66 for Heat Transformation and Heat Storage Applications. *Dalton Trans.* **2013**, *42* (45), 15967–15973.

(22) Canivet, J.; Fateeva, A.; Guo, Y.; Coasne, B.; Farrusseng, D. Water Adsorption in MOFs: Fundamentals and Applications. *Chem. Soc. Rev.* **2014**, *43*, 5594–5617.

(23) Coasne, B.; Gubbins, K. E.; Pellenq, R. J. M. Temperature Effect on Adsorption/Desorption Isotherms for a Simple Fluid Confined within Various Nanopores. *Adsorption* **2005**, *11*, 289–294.

(24) Jasuja, H.; Zang, J.; Sholl, D. S.; Walton, K. S. Rational Tuning of Water Vapor and CO_2 Adsorption in Highly Stable Zr-Based MOFs. *J. Phys. Chem. C* **2012**, *116* (44), 23526–23532.

(25) Burtch, N. C.; Jasuja, H.; Walton, K. S. Water Stability and Adsorption in Metal − Organic Frameworks. *Chem. Rev.* **2014**, *114* (20), 10575–10612.

(26) Furukawa, H.; Gándara, F.; Zhang, Y.-B.; Jiang, J.; Queen, W. L.; Hudson, M. R.; Yaghi, O. M. Water Adsorption in Porous Metal-Organic Frameworks and Related Materials. *J. Am. Chem. Soc.* **2014**, *136* (11), 4369–4381.

(27) Rieth, A. J.; Tulchinsky, Y.; Dincă, M. High and Reversible Ammonia Uptake in Mesoporous Azolate Metal-Organic Frameworks with Open Mn, Co, and Ni Sites. *J. Am. Chem. Soc.* **2016**, *138* (30), 9401–9404.

(28) Liao, P.-Q.; Li, X.-Y.; Bai, J.; He, C.-T.; Zhou, D.-D.; Zhang, W.-X.; Zhang, J.-P.; Chen, X.-M. Drastic Enhancement of Catalytic Activity via Post-Oxidation of a Porous MnII Triazolate Framework. *Chem. - Eur. J.* **2014**, *20* (36), 11303–11307.

(29) Liao, P.-Q.; Chen, H.; Zhou, D.-D.; Liu, S.-Y.; He, C.-T.; Rui, Z.; Ji, H.; Zhang, J.-P.; Chen, X.-M. Monodentate Hydroxide as a Super Strong yet Reversible Active Site for CO_2 Capture from High-Humidity Flue Gas. *Energy Environ. Sci.* **2015**, *8* (3), 1011–1016.

(30) Rieth, A. J.; Dincă, M. Controlled Gas Uptake in Metal-Organic Frameworks with Record Ammonia Sorption. *J. Am. Chem. Soc.* **2018**, *140* (9), 3461–3466.

(31) Derouane, E. G.; Chang, C. D. Confinement Effects in the Adsorption of Simple Bases by Zeolites. *Microporous Mesoporous Mater.* **2000**, *35–36* (1387), 425–433.

(32) de Lange, M. F.; van Velzen, B. L.; Ottevanger, C. P.; Verouden, K. J. F. M.; Lin, L.-C.; Vlugt, T. J. H.; Gascon, J.; Kapteijn, F. Metal–Organic Frameworks in Adsorption-Driven Heat Pumps: The Potential of Alcohols as Working Fluids. *Langmuir* **2015**, *31* (46), 12783–12796.

DOI: 10.1021/jacs.8b09655
J. Am. Chem. Soc. 2018, 140, 17591–17596

(33) Carter, J. W.; Wyszynski, M. L. The Pressure Swing Adsorption Drying of Compressed Air. *Chem. Eng. Sci.* **1983**, *38* (7), 1093−1099.

DOI: 10.1021/jacs.8b09655
J. Am. Chem. Soc. 2018, 140, 17591−17596